Journal of Advanced Research 36 (2022) 39–49

Contents lists available at ScienceDirect

Journal of Advanced Research

journal homepage: www.elsevier.com/locate/jare

# Eco-friendly surface modification approach to develop thin film nanocomposite membrane with improved desalination and antifouling properties

Ying Siew Khoo [a], Woei Jye Lau [a,*], Yong Yeow Liang [b], Mustafa Karaman [c], Mehmet Gürsoy [c], Ahmad Fauzi Ismail [a]

[a] Advanced Membrane Technology Research Centre (AMTEC), Universiti Teknologi Malaysia, 81310 Johor Bahru, Johor, Malaysia
[b] Faculty of Chemical and Process Engineering Technology, College of Engineering Technology, Universiti Malaysia Pahang, Lebuhraya Tun Razak, 26300 Gambang, Kuantan, Pahang, Malaysia
[c] Department of Chemical Engineering, Konya Technical University, Konya 42075, Turkey

## HIGHLIGHTS

- Rapid and environmentally friendly method for surface modification of thin film nanocomposite (TFN) membrane.
- The developed surface-modified TFN membrane also exhibited remarkable antifouling property and flux recovery rate (>95%).
- NaCl passage reduced from 2.43% to 1.50% without significantly altering pure water flux.

## GRAPHICAL ABSTRACT

Illustration of AA-modified TFN membrane embedded with surface-modified TNTs.

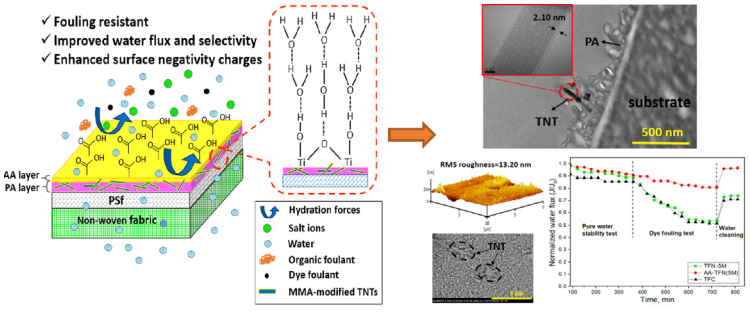


## ARTICLE INFO

*Article history:*
Received 15 January 2021
Revised 2 June 2021
Accepted 5 June 2021
Available online 15 June 2021

*Keywords:*
Plasma modification
Thin film nanocomposite
Hydrophilic acrylic acid
Nanotechnology
Desalination

## ABSTRACT

*Introduction:* Nanomaterials aggregation within polyamide (PA) layer of thin film nanocomposite (TFN) membrane is found to be a common issue and can negatively affect membrane filtration performance. Thus, post-treatment on the surface of TFN membrane is one of the strategies to address the problem.
*Objective:* In this study, an eco-friendly surface modification technique based on plasma enhanced chemical vapour deposition (PECVD) was used to deposit hydrophilic acrylic acid (AA) onto the PA surface of TFN membrane with the aims of simultaneously minimizing the PA surface defects caused by nanomaterials incorporation and improving the membrane surface hydrophilicity for reverse osmosis (RO) application.
*Methods:* The TFN membrane was first synthesized by incorporating 0.05 wt% of functionalized titania nanotubes (TNTs) into its PA layer. It was then subjected to 15-s plasma deposition of AA monomer to establish extremely thin hydrophilic layer atop PA nanocomposite layer. PECVD is a promising surface modification method as it offers rapid and solvent-free functionalization for the membranes.
*Results:* The findings clearly showed that the sodium chloride rejection of the plasma-modified TFN membrane was improved with salt passage reduced from 2.43% to 1.50% without significantly altering

Peer review under responsibility of Cairo University.
* Corresponding author.
*E-mail address:* lwoeijye@utm.my (W.J. Lau).

https://doi.org/10.1016/j.jare.2021.06.011
2090-1232/

pure water flux. The AA-modified TFN membrane also exhibited a remarkable antifouling property with higher flux recovery rate (>95%, 5-h filtration using 1000 mg/L sodium alginate solution) compared to the unmodified TFN membrane (85.8%), which is mainly attributed to its enhanced hydrophilicity and smoother surface. Furthermore, the AA-modified TFN membrane also showed higher performance stability throughout 12-h filtration period.

*Conclusion:* The deposition of hydrophilic material on the TFN membrane surface via eco-friendly method is potential to develop a defect-free TFN membrane with enhanced fouling resistance for improved desalination process.



## Introduction

Since the first report on the fabrication of reverse osmosis (RO) thin film nanocomposite (TFN) membrane was published in 2007 by Jeong et al. [1], a wide range of inorganic nanofillers (e.g., titanium dioxide ($TiO_2$), graphene oxide (GO), carbon nanotube (CNT), titania nanotube (TNT), zinc oxide (ZnO) and silicon dioxide ($SiO_2$)) with different characteristics were used by membrane scientists as alternative promising materials to improve the TFN membrane performance for both pressure-driven and osmotically-driven filtration processes [2,3]. Membrane scientists always reported the improved surface properties of resultant membranes upon the nanofillers incorporation. These include better water flux and/or selectivity [4,5], improved antifouling behaviour [6], enhanced chlorine resistivity [7] as well as better mechanical stability [8].

To fabricate TFN membranes, two main approaches, i.e., surface deposition/layer-by-layer (LbL) self-assembly [9–11] and interfacial polymerization (IP) can be employed to introduce the nanomaterials into the polyamide (PA) selective layer of the membrane. The surface deposition of nanomaterials on the membrane can be attained through mechanisms such as chemical/physical interaction and electrostatic interaction [12]. This method allows the introduction of desired functional groups to improve the existing membrane surface characteristics without changing the intrinsic properties of PA selective layer. Moreover, the presence of nanomaterials-coated layer atop the PA could act as a protective film to the underlying cross-linked selective layer [13]. However, this method encounters a major drawback which is high tendency of nanomaterials detachment/leaching during filtration process.

Previously, Kim et al. [11] deposited CNTs onto the PA surface followed by polyvinyl alcohol (PVA) coating, but reported that CNTs could still be detected in the feed solution during membrane operation. This is most likely due to the weak physical bonding of loosely attached CNTs on the membrane surface. Similarly, Isawi et al. [9] found out that 3.32% of Zn ions were leached out from the ZnO-incorporated TFN membrane after 10-day placing it in 1-L distilled water (DI) via batch experiment. The leaching of Zn ions is likely ascribed to the dissolution of unreacted ZnO appeared on the PA surface. Furthermore, the existence of hydrodynamic shear stress during filtration process could be another reason that causes detachment of nanomaterials and diminishes the TFN membrane performance and stability [10,14]. For instance, the silver (Ag) nanoparticles-coated PA layer as developed by Park et al. [14] via plasma surface deposition was reported to have 30% of weakly-bound Ag nanoparticles detached from the PA layer after 24-h testing in a highly-pressurized shear flow condition.

Besides surface deposition of nanomaterials, the TFN membranes made of IP technique by introducing nanomaterials into either aqueous or organic monomer solution also encounter nanofillers leaching issue [12,15,16]. However, hydrophilic nanomaterials are not able to disperse well in non-polar solvents and this poses a great challenge in producing a homogenous mixture for PA nanocomposite layer synthesis. Although dispersing hydrophilic nanomaterials in aqueous solution seem to be more practical, this approach has its own downside. The requirement of removing excess aqueous solution from the substrate during IP process could result in large amount of nanomaterials being rolled out together with the excess amine solution, leaving only few quantity of nanomaterials in the resultant TFN membrane [17].

Although better dispersion of nanomaterials in the organic solution can be achieved upon surface modification/functionalization of nanomaterials, its agglomeration could not be completely eliminated due to the presence of van der Waals attractive force between nanoparticles that tend to form agglomerates especially at high loading [4,18]. The aggregation of nanomaterials witin the PA matrix might develop defects (hole/voids), leading to a decreased salt removal rate [19,20]. Emadzadeh et al. [21] reported NaCl rejection of RO membrane was greatly attenuated from 94.05% to 85.87% upon incorporation of 0.1 wt% nanofillers into the PA layer, although flux was increased. Dong et al. [22] and Ghanbari et al. [23] also found lower selectivity of TFN membranes against NaCl and attributed it to the aggregation of nanomaterials that developed imperfection in the PA layer. To overcome the PA surface defects caused by the embedded nanomaterials, Chong et al. [24] modified the surface of TNTs using a silane coupling agent – N-(2-Aminoethyl)-3-aminopropyltrimethoxysilane (AAPTS) to improve the dispersion stability followed by coating a thin PVA layer atop the TFN membrane with the aim of healing the imperfection. Besides being able to improve the membrane NaCl rejection by up to 9%, the presence of PVA layer also rendered higher resistance degree against foulants owing to its hydrophilic nature. However, silane couling agent that made up of amino groups and ethoxy groups is highly hazardous and harmful to environment [25]. With respect to conventional surface coating technique, the presence of relatively thick coating layer could compromise the water permeation of membrane owing to the increase in water transport resistance [26]. For the chemical grafting, the process requires chemical initiators to generate free radicals [27] and the desired grafting degree somehow is difficult to achieve due to the complex mechanism [28].

Inspired by the advantages of surface coating and nanoparticle incorporation, this study aims to integrate both techniques to produce TFN membrane with minimum surface defects for RO application by employing rapid surface deposition technique – plasma enhanced chemical vapour deposition (PECVD) to form a hydrophilic thin layer atop nanofiller-incorporated PA layer. The TFN membrane was first synthesized by introducing surface-functionalized TNTs into the PA layer via IP technique. We employed PECVD technique to deposit a thin film polymeric layer of methylmethacrylate (MMA) ($CH_2$=$CCOOCH_3$) on the surface of TNTs to improve its dispersion behaviour in non-polar solvent. The use of MMA for surface modification of nanofillers is due to its hydrophobic nature and high degree of biocompatibility that are effective to enhance the nanofiller dispersion in non-polar solvent [29]. The TNTs-incorporated TFN membrane was further modified by PECVD

technique to form a hydrophilic polyacrylic acid (PAA) atop selective layer to improve the surface properties and heal possible surface defects existed on the TFN membrane. Such coating approach is expected to avoid the leaching of TNTs from the membrane. PECVD method is employed for the surface modification of both nanomaterials and TFN membrane because it can alter the material surface functionality [30] with its lower degree of plasma ionization without damaging the bulk material [31]. Furthermore, this technique offers fast reaction time and does not require any hazardous materials like the conventional surface grafting and coating methods [32]. In this work, self-synthesized TFC membrane and one commercial TFC RO membrane were also surface-modified by PECVD and served as control samples to evaluate the efficiency of the developed TFN membrane. All of the membranes were subjected to a series of instrumental characterization followed by filtration analyses that include water flux, salt rejection, antifouling properties and performance stability.

## Experimental

### *Synthesis and surface modification of TNTs*

In this work, alkaline hydrothermal method reported by Subramaniam et al. [33] was employed for the synthesis of TNTs. Briefly, 3 g of titanium dioxide ($TiO_2$, Degussa P25 from Evonik Industries) nanoparticles was first mixed with 120-mL aqueous solution containing 10 M sodium hydroxide (NaOH, Fisher Scientific) at 25 °C for 4 h. Next, the suspension was poured into a 200-mL Teflon autoclave and heated overnight in an oven at 180 °C. The autoclave was allowed to cool down to room temperature after completing heating process. The white powder inside the autoclave was collected via centrifugal process. The powder was then repeatedly rinsed with RO water (produced by Milli-Q® Ultrapure Water System) followed by 0.1 M hydrochloric acid (HCl, 37%, ACS reagent) until the pH of decanter water close to 7. The TNTs in white powder form were then separated using filter paper and dried at 60 °C to completely remove water.

The surface of synthesized TNTs was further functionalized using a rotating-bed PECVD system with procedure similar to the work of Gürsoy and Karaman [34]. In brief, a cylindrical Pyrex tube (diameter: 6 cm) was adopted as a vacuum reactor and inductively joined by copper antenna connected to a plasma generator with 13.56 MHz radio frequency (RF). The vacuum compatible ferrofluidic rotary feedthroughs were placed at both sides of the Pyrex reactor in order to achieve vacuum condition. Then, MMA (99%, Sigma Aldrich) monomer was vaporized in a steel jar at room temperature followed by feeding it into the vacuum reactor at a flow rate of 1.5 sccm. The reaction time between MMA and TNTs was fixed at 5 min. After the reaction was complete, the plasma was turned off and the MMA-modified TNTs was collected from the Pyrex reactor. The MMA-modified TNTs could be directly used for TFN membrane fabrication without further post-treatment.

### *Fabrication and surface modification of membranes*

The procedure of membrane fabrication conducted in this work was similar to our previously published work [35]. Selective layer of composite membranes was fabricated through conventional IP technique on the polysulfone (PSf) microporous substrate (PS20, RisingSun Membrane Technology (Beijing) Co. Ltd., China). Prior to the IP process, the PSf substrate was first immersed in the RO water overnight to eliminate gylcerin from its surface. Subsequently, the PSf substrate (14 cm × 14 cm) was clamped between a rubber gasket and rectangle acrylic frame. A 40-mL aqueous solution containing 2 wt% m-phenylenediamine (MPD, 98%, Merck), 1 wt% (+)−10−camphorsulfonic acid (CSA, 99%, Sigma Aldrich), 1 wt% triethylamine (TEA, >99%, Sigma Aldrich) and 0.05 wt% sodium dodecyl sulfate (SDS, Merck) was carefully poured onto the surface of substrate and remained for 3 min before draining off using a rubber roller. 20 mL of 0.1 wt% trimesoyl chloride (TMC, 98%, Acros Organics) in Isoparaffin-G (Isopar, Exonmobil) was introduced onto the MPD-saturated substrate surface and allowed to polymerize with MPD for 1 min. The excess TMC organic solution was then poured off and the membrane surface was rinsed with 30-mL n-hexane (>98%, Merck) to remove the unreacted monomers, followed by heat treatment in oven at 60 °C for 20 min. The fabrication of TNT-incorporated PA layer for TFN membrane was similar to the aforementioned procedure, except a fixed amount of 0.05 wt% MMA-modified TNTs was dispersed in the TMC solution. Hereafter, the membrane without nanomaterials is denoted as TFC while the membrane incorporated with 0.05 wt% MMA-modified TNTs is referred as TFN(5M).

To modify the top surface of PA layer, the prepared TFC and TFN membranes were respectively transferred onto a substrate holder located within a cylindrical Pyrex tube PECVD reactor as illustrated in Fig. 1. The back side of substrate holder was equipped with a water circulating chiller (Thermo Neslab) to maintain the sample temperature throughout the modification period. A plasma generator RF was connected to the PECVD reactor via a copper coil antenna to generate 40-W plasma at 13.56 MHz. A rotary-vane vacuum pump (Edwards XDS-10) was applied to the reactor to create a vacuum environment while the pressure in the reactor was monitored by a capacitance type manometer. Acrylic acid (AA, 99%, Sigma Aldrich) was first vaporized in a stainless-steel jar at 60 °C via a heating tape controlled by PID temperature controller. Thereafter, the vaporized AA was delivered into the reactor chamber through a needle valve and the reaction time was fixed at 15 s. After completing the reaction, the reactor power was immediately turned off and the surface-modified membrane was collected. Hereafter, the surface-modified membranes are symbolized as AA-TFC and AA-TFN(5M) membrane. In this work, a commercial RO membrane - XLE from Dow FilmTec (USA) was also modified by AA and used to benchmark with the self-synthesized membranes. The commercial membrane before and after AA modification is denoted as XLE and AA-XLE, respectively.

### *Characterization of TNTs*

The crystalline characteristics of self-synthesized TNTs and MMA-modified TNTs were investigated via D-Max Rigaku diffractometer at a scan speed of 8.2551°/min, scanned from 10° to 80° (2θ) under operating conditions of 40 kV and 30 mA. The functional groups of pristine and surface-modified TNTs were recorded using Fourier transform infrared (FTIR) spectrometer (Perkin Elmer Spectrum, Frontier) with wavenumber ranged from 600 to 4000 $cm^{-1}$ using pressed potassium bromide (KBr) pellet method. High resolution-transmission electron microscopy (HR-TEM) analysis was performed using JEM-ARM 200F (JEOL) at 200 kV to study the structure of nanomaterials. Prior to the TEM sample view, small amount of nanomaterials was dispersed in ethanol solution followed by sonication for 30 min before transferring it onto a copper grid.

### *Characterization of membranes*

The chemical functional groups of membranes were detected using attenuated total reflection-Fourier transform infrared (ATR-FTIR) spectroscope (Thermo Scientific, Nicolet 5700) in the range of 400–4000 $cm^{-1}$. The membranes were dried in an oven at 40 °C for 24 h prior to FTIR analysis to eliminate the membrane moisture. The surface roughness of membranes was characterized

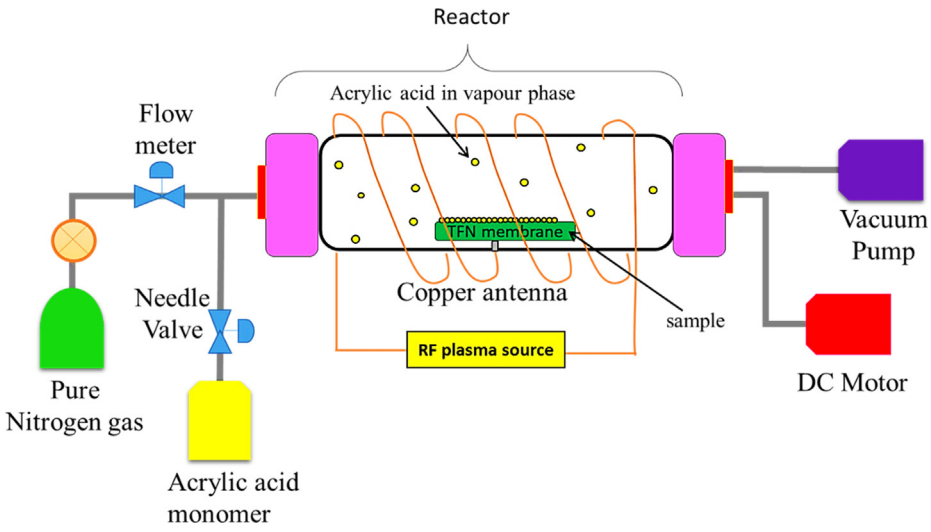


**Fig. 1.** Schematic diagram of PECVD system for TFN membrane surface modification.

using atomic force microscope (AFM) (Hitachi, AFM5000 II) with a scan size of 10 μm × 10 μm at non-contact mode. The membrane surface hydrophilicity was evaluated via sessile drop method using a contact angle goniometer (DataPhysics, OCA 15Plus). 0.5-μL water was dropped down on the flat membrane surface with RO water was used as probe liquid. At least ten water contact angle (WCA) measurements were taken to yield an average result. The presence of MMA-modified TNTs within the PA layer was visualized using TEM (Hitachi, HT7700) at 120 kV. Prior to TEM analysis, the TFN membrane was embedded in the epoxy resin (Eponate 12, Ted Pella. Inc.) for overnight and the resultant resin block was then sliced to a thickness of 50 nm using PowerTome ultramicrotome (RMC Boeckeler). The surface morphology and cross-sectional structure of membranes were visualized using field emission scanning electron microscope (FESEM) (Hitachi, SU8000). Prior to FESEM analysis, a small piece of membrane sample was fractured in the liquid nitrogen followed by placing it onto the stub using carbon tap [36]. A thin gold film was sputter-coated on the sample surface to avoid charging effect during FESEM scanning. The energy dispersive X-ray (EDX) spectroscope (Oxford, Xmax-N 50 mm) attached to the FESEM was used for elemental mapping analysis. An electrokinetic analyser (Anton Paar, SurPASS™) was used to determine the surface charge of membrane. Membrane zeta potential was determined as a function of pH (between pH 2.0 and pH 10.5) via pH titration using 0.05M of HCl and 0.05M of NaOH solution. 1 millimolar of KCl solution was used as background electrolyte during electrokinetic analysis. ImageJ software was used to measure the PA layer thickness and to estimate the voids area (%) of PA layer based on the TEM images.

*Membrane performance evaluation*

The membrane filtration experiments were implemented using a commercial dead-end filtration cell (Sterlitech™, HP4750). The stainless steel stirred cell is chemical and solvent resistant and has an active membrane filtration area of 14.6 $cm^2$. All experiments of pure water flux (PWF) and NaCl separation efficiency were conducted at the stirring speed of 360 rpm. The membrane was first compacted at 16 bar for a duration of 30 min, followed by 15 bar for 15 min before any measurement was started to take. At least three measurements were taken for each membrane coupon to yield an average result. Herein, the membrane PWF, J ($L/m^2$. h) was calculated by following equation:

$$J = \frac{\Delta V}{A_m \Delta t} \quad (1)$$

where $A_m$, ΔV and Δt represent effective membrane area ($m^2$), permeate volume (L) and permeate collection time (h), respectively. Meanwhile, the salt passage of membrane (P, %) tested using 2000 mg/L NaCl (Merck) at 15 bar was evaluated using:

$$P = \frac{C_p}{C_F} \times 100 \quad (2)$$

where $C_p$ is the solute concentration in permeate solution and $C_F$ is the solute concentration in feed solution.

The rejection of membranes against Reactive Black 5 (RB5, MW = 991 g/mol, Sigma-Aldrich) was also evaluated under 1000 ppm of RB5 feed solution with the constant stirring speed of 360 rpm at 15 bar. The dye concentrations in the feed and permeate solutions were measured using UV–vis spectrophotometer (Hach, DR5000) at specific wavelength of RB5 solution.

*Antifouling and stability test*

Membrane fouling test was conducted using 1000 mg/L sodium alginate solution (NaAlg, Sigma Aldrich) under 15 bar and 360 rpm stirring speed for 5 h. The decline trend of normalized PWF ($J/J_o$) graph was plotted to investigate the fouling behaviour of the surface-modified and unmodified membrane in which J represents the final PWF while $J_o$ represents the initial PWF of membrane. After 5-h fouling filtration test, the NaAlg solution was replaced with 300-mL RO water and the fouled membrane was allowed to rinse about 15 min before its PWF was re-measured. The flux recovery rate (FRR, %) of the membranes can be determined using the following equation:

$$FRR = \left(\frac{J_2}{J_1}\right) \times 100 \quad (3)$$

where $J_1$ is the initial PWF of virgin membrane and $J_2$ is PWF of rinsed membrane after being tested with NaAlg solution.

Stability test was also conducted for TFC, TFN(5M) and AA-TFN (5M) membranes by subjecting the used membranes to continuous dye fouling filtration. First and foremost, 300 mL of RO water was introduced into the filtration cell, followed by membrane compression at 16 bar for 30 min at 360 rpm. Then, the membrane PWF was recorded every 30 min with a total filtration period of 6 h at 15 bar. In order to evaluate the stability of membrane, the same mem-

brane was subjected to a prolonged dye filtration test (up to 6 h). A 300-mL feed solution containing 1000 ppm RB5 was poured into the filtration cell and the water flux change was recorded every 30 min. Subsequently, RO water was used to rinse the fouled membrane to obtain the FRR. Normalized flux of membrane ($J/J_o$) against time was then plotted to access the extend of membrane stability. The FRR after RB5 fouling test can be calculated using Eq. (3) aforementioned.

*Leaching test*

The possible leaching of TNTs from the TFN(5M) and AA-TFN (5M) membrane was evaluated by measuring the water samples collected from the feed and permeate solution of the respective membrane every 2 h for up to 8 h. 300 mL of RO water was used as feed solution throughout the filtration test and the operating pressure was fixed at 15 bar. The RO water inside the dead-end cell was replaced after the feed and permeate samples were collected every 2 h. The presence of titanium (Ti) element in the feed and permeate samples were then analyzed using inductively coupled plasma mass spectrometer (ICP-MS) (Perkin Elmer, NEXION 2000).

## Results and discussion

*Characterization of MMA-modified TNTs*

The TEM images as shown in Fig. 2(a) indicate that a thin film layer with thickness of ~2 nm can be clearly seen on the surface of TNTs when compared to the pristine TNTs (Fig. S1(a)). This thin layer is corresponded to the polymerized MMA that was developed upon PECVD process. It is also found that the self-synthesized TNTs exhibit open-ended tubular shape with diameter in the range of 24–28 nm as measured by ImageJ. With respect to its surface chemistry, the stronger broad band between 3100 $cm^{-1}$ and 3500 $cm^{-1}$ as shown in the modified TNTs in Fig. 2(b) clearly implies the presence of hydroxyl functional groups of TNTs. It must be noted that additional peaks occurred at 1630 $cm^{-1}$ (C=C stretching), 1446 $cm^{-1}$ ($CH_3$ stretching) and 1143 $cm^{-1}$ (C-O bending) for the MMA-modified TNTs are strong evidence of the presence of MMA in the nanomaterials. With respect to the crystallinity, Fig. 2(c) shows that three important XRD peaks of TNTs (i.e., 10.90°, 24.70° and 48.50°) remain unchanged even after it was surface-modified. This confirms that mild surface modification using polymer does not alter the crystallinity of TNTs. These three XRD peaks are corresponded to the diffraction index of TNTs at (2 0 0), (1 1 0) and (0 2 0), respectively [17]. It is also found that the MMA-modified TNTs demonstrate better dispersion in IsoparG solution than that of pristine TNT as shown in Fig. S1(b). This indicates that the hydrophobic coating could effectively enhance the dispersion of TNTs in non-polar solvent by hindering the strong van der Waals attractive force between nanofillers and reducing severe aggregation in the solvent.

*Characterization of membranes*

Fig. 3 compares the FTIR spectrum of TFC and TFN membranes with and without plasma modification. The changes on the surface functional groups of commercial XLE membrane before and after AA deposition can also be found in Figure S2. Typical peaks due to the PA layer are noticed at 1660 $cm^{-1}$ and 1540 $cm^{-1}$ for all the composite membranes and they are corresponded to C=O stretching vibration (amide I) and N–H stretching (amide II), respectively. In addition to the PA selective layer, O=S=O stretching vibration that belongs to PSf substrate is also detected at 1150 $cm^{-1}$. It is worth noting that a stronger peak intensity at 1710 $cm^{-1}$ and 1250 $cm^{-1}$, referring to C=O stretching (carboxyl group) and C–O–H stretching vibration, respectively can be observed for the AA-TFC and AA-TFN(5M) membranes. This clearly indicates the successful AA deposition atop the PA layer. All of the AA-modified membranes also show significant broad peak at 3300 $cm^{-1}$, which is contributed by the –OH functional group of AA [37]. It must be noted that the peaks at 1040 $cm^{-1}$ and 930 $cm^{-1}$ which correspond to C-O and C=$CH_2$ groups, respectively are obvious for the AA-modified membranes and this might be due to the presence of unreacted AA monomer on the membrane surface.

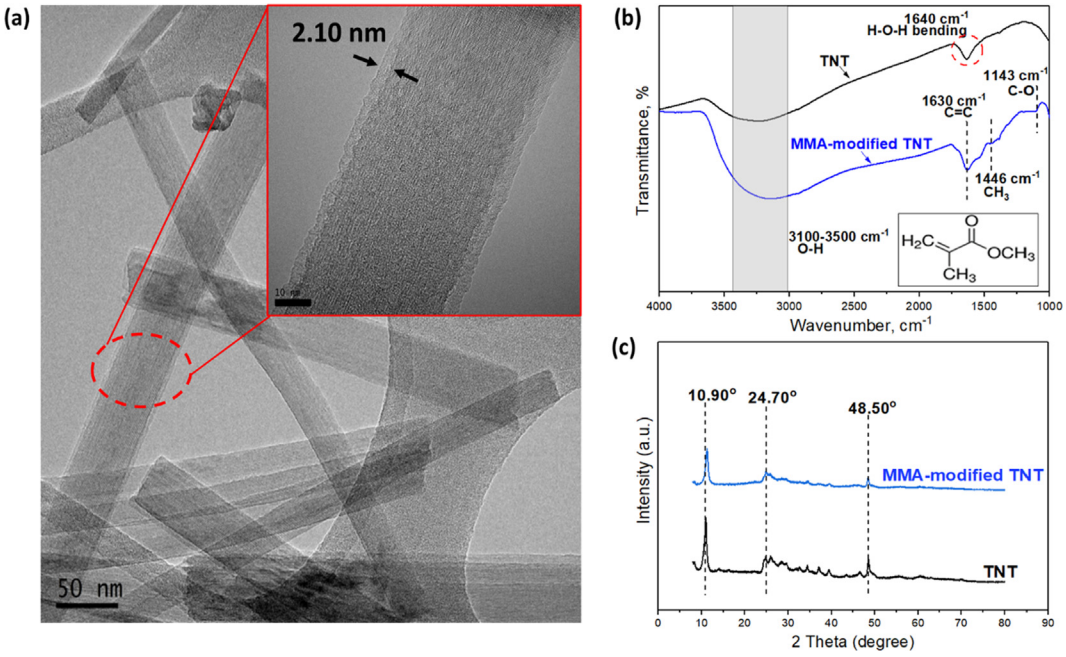


**Fig. 2.** (a) TEM image for MMA-modified TNTs (Inset: MMA-modified TNTs image at scale bar of 10 nm) and properties of unmodified and MMA-modified TNTs, (b) FTIR spectra (Inset: Organic structure of MMA) and (c) XRD analysis.

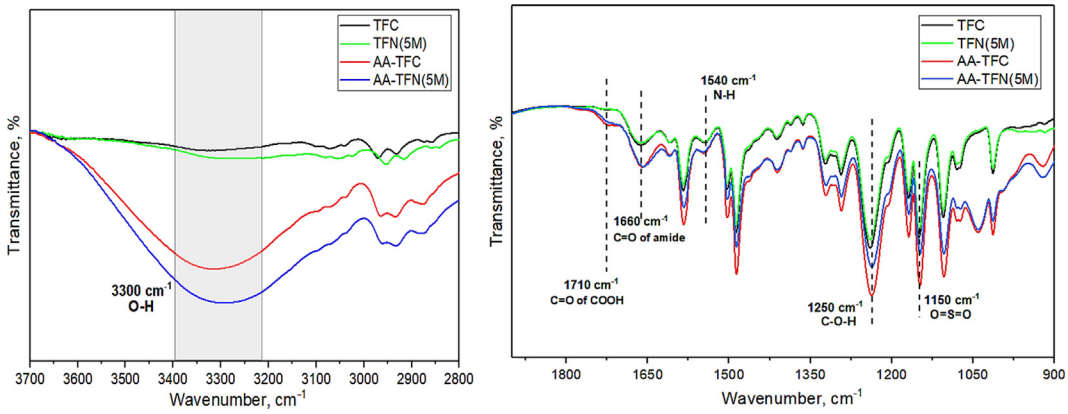


**Fig. 3.** ATR-FTIR spectra of different composite membranes, (a) 3700 to 2800 $cm^{-1}$ and (b) 1900 to 900 $cm^{-1}$.

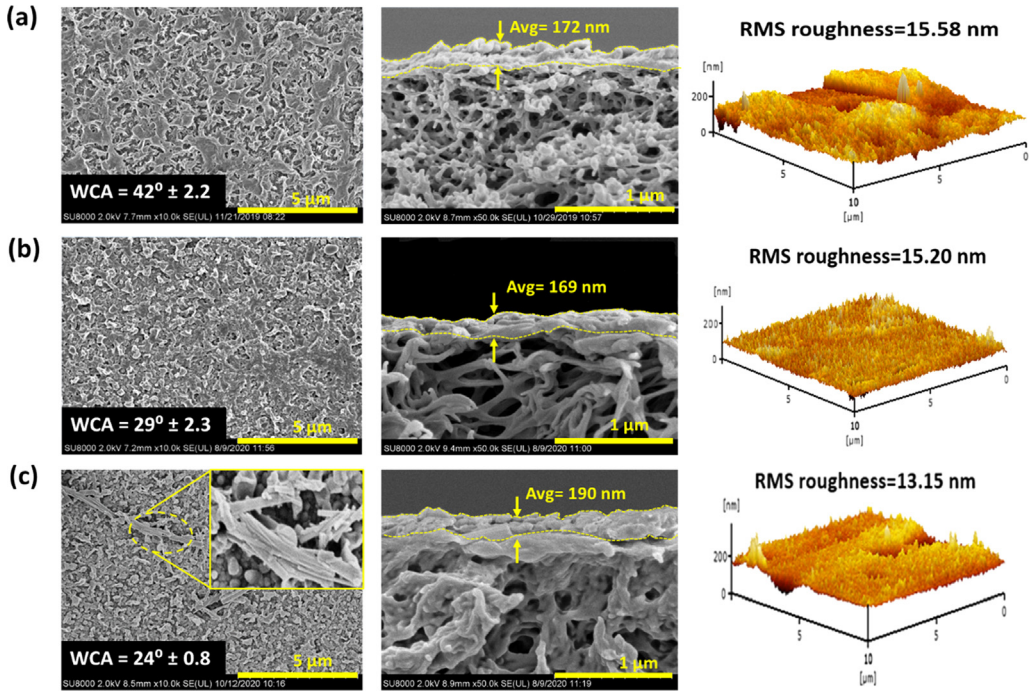


**Fig. 4.** Surface morphology (left) and cross-sectional structure (middle) of membranes examined under FESEM and their respective 3D AFM image (right), (a) AA-XLE, (b) AA-TFC and (c) AA-TFN(5M) membranes shows the MMA-modified TNTs embedded within PA layer). Note: WCA of each membrane is also presented.

The surface wettability of the fabricated membranes was further investigated through the WCA analysis. It is found that all of the AA-modified membranes exhibit significantly lower WCA (Fig. 4) than those of unmodified membranes (Fig. S3). The introduction of carboxylic acid (–COOH) and hydroxyl (–OH) functional groups on the membrane surface by the AA plasma deposition has effectively increased the membrane hydrophilicity, making it to have better water affinity. The AA-TFN(5M) membrane in particular displays the lowest WCA. This is owing to the embedment of hydrophilic nanomaterials within the PA matrix that make the membrane to have higher water affinity.

Fig. 4 also compares the surface and cross-sectional morphology of FESEM images and 3D AFM images of three different AA-modified membranes. The surface structure of unmodified membranes are also examined and the images can be viewed in Fig. S3. Overall, all these composite membranes possess ridge and valley structure on their respective surface, which is typically found in the PA layer synthesized via MPD and TMC monomers [38,39]. Two distinct differences of the AA-modified membranes compared to the unmodified membranes are the increase in selective layer thickness and decrease in surface roughness. For instance, the thickness of the TFN(5M) membrane is increased from 132.7 to 190.0 nm while its RMS roughness is reduced from 14.54 to 13.20 nm upon the AA deposition. The results can be attributed to the formation of additional layer that covers the valleys of PA layer, making it to become smoother. Similar results were also reported by Liu et al. [40] and Abbas et al. [41] in which the membrane surface roughness was reduced after the AA surface coating.

By comparing between the AA-modified membranes, the AA-TFN(5M) membrane possesses the thickest selective layer (190.0 nm) compared to the AA-XLE and AA-TFC membrane. This is likely due to the presence of nanomaterials during IP process that retains excess aqueous monomers and results in rougher membrane surface. The existence of excess MPD is able to cross-link with TMC, forming thicker PA structure [42]. With respect to

surface roughness, all the AA-modified membranes exhibit very similar RMS value (in the range of 13.15–15.58 nm) as the additional PAA layer deposited on these membrane surfaces was performed under the same PECVD conditions. The existence of modified TNTs on the surface of AA-TFN(5M) membrane is further examined via EDX analysis and the detection of titanium (Ti) in the EDX mapping and element composition as shown in Fig. S4 and Table S1, respectively is the strong evidence to confirm the existence of TNTs in the membrane sample.

Fig. 5 compares the cross-sectional TEM image of AA-TFN(5M) membrane with TFN(5M) membrane. For both membranes, it can be clearly observed that the nanomaterials are located near to the surface of ridge-and-valley PA, confirming the existence of TNTs (with or without modification) within the selective layer. For the TFN(5M) membrane, its PA layer is estimated to have ~1.65% voids area. The impregnation of hydrophilic nanomaterials that tends to accelerate the aqueous diffusion into organic solution by attracting water molecules from amine-saturated substrate via hydrogen bonding could lead to voids formation as explained elsewhere [4,43]. Another factor that can develop voids is due to the aggregation of nanomaterials that limits the MPD to react with TMC during IP process, thus interrupting PA cross-linking [44]. It is worth noting that the voids fraction is significantly reduced upon the AA deposition as evidenced in the AA-TFN(5M) membrane. For this membrane, its AA-modified PA layer is estimated to have ~0.67% of voids area. The reduced voids fraction can also be corresponded to the reduced selective layer defects which form a membrane with enhanced separation rate. Additionally, the average PA layer thickness of TFN(5M) (~130 nm) and AA-TFN(5M) (~193 nm) membrane as shown in the TEM images is in good agreement with the thickness measured based on FESEM images.

*Membrane filtration*

Fig. 6 compares the RO performance of different AA-modified membranes. Noticeably, both AA-TFC and AA-TFN(5M) membranes demonstrate higher water flux and lower NaCl passage compared to the commercial AA-XLE membrane. The order of the water flux is AA-TFN(5M) > AA-TFC > AA-XLE. More specifically, the water flux of AA-TFN(5M) membrane is 11.7% and 15.7% higher than those of AA-TFC and AA-XLE membrane, respectively. The promising performance of AA-TFN(5M) membrane can be explained by the fact that the deposition of hydrophilic polymer onto the PA surface coupled with the embedment of MMA-modified TNTs within the PA matrix are the key factors leading to improved membrane surface hydrophilicity by faciliting water molecules to diffuse through the membrane [32,45]. The improved surface hydrophilicity has been proved by the presence of hydroxyl functional group as shown in Fig. 3 and reduced WCA in Fig. 4. Other than that, studies have shown that embedding hollow nanomaterials within PA layer could further act as an additional effect in promoting water flux [21,24]. With respect to separation performance, the AA-TFN(5M) membrane shows remarkable NaCl rejection with only 1.5% (35.54 ppm) of dissolved ions diffuse through the membrane. As a comparison, the AA-XLE and AA-TFC membranes record 2.9% (54.63 ppm) and 2.5% (52.48 ppm) salt passage, respectively. It is believed that the interaction between water molecules and metal-hydroxyl group of TNTs via hydrogen bonding could form a hydration layer which minimizes dissolved ions to pass through the membrane [46].

In comparison with the membranes without AA modification as reported in our previous study [35], the AA-XLE, AA-TFC and AA-TFN(5M) membranes are reported to experience 65.7%, 3.8% and 5.7% reduction in water flux, respectively. This can be ascribed to the additional thin film deposited on the PA surface that creates hydraulic resistance for water transportation and surpasses the positive effect of enhanced membrane hydrophilicity [32,47]. Similar findings were also reported by Chong et al. [24] and Vatanpour and Zoqi [48] in which the water flux of their developed TFC membrane was adversely affected after PVA and AA were respectively deposited on the membrane surface. Nevertheless, it must be pointed out that the presence of AA layer on the membranes as shown in our work is found to be positive in improving salt rejection as the voids of selective layer is partially filled by the AA during plasma process. This, as a result, develops a denser PA layer that is more effective to retain NaCl[49].

The separation efficiency of AA-XLE, AA-TFC and AA-TFN(5M) membranes are higher compared to their respective unmodified membranes, recording a reduction of salt passage from 12.9% to 2.9%, from 3.5% to 2.5% and from 2.43% to 1.5%, respectively. The sealing of voids or defects caused by the embedment of nanofillers and the coverage of nanofillers' channel by AA modification could be the possible reasons for reducing ions passage through membrane [24,50,51]. Meanwhile, the enhanced surface negativity of AA-modified membranes based on the zeta potential analysis as shown in Fig. S5 could be one of the reasons contributing to lower salt passage. The increase in surface charge from –20 mV (at pH 6.7) in the unmodified TFN(5M) membrane to –40 mV in the AA-modified TFN(5M) membrane can be related to the presence of –COOH group of coating material on the modified membrane surface. Subsequently, the electrostatic repulsion force between dissolved ions and AA-TFN(5M) membrane becomes stronger which results in lower salt passage through the membrane.

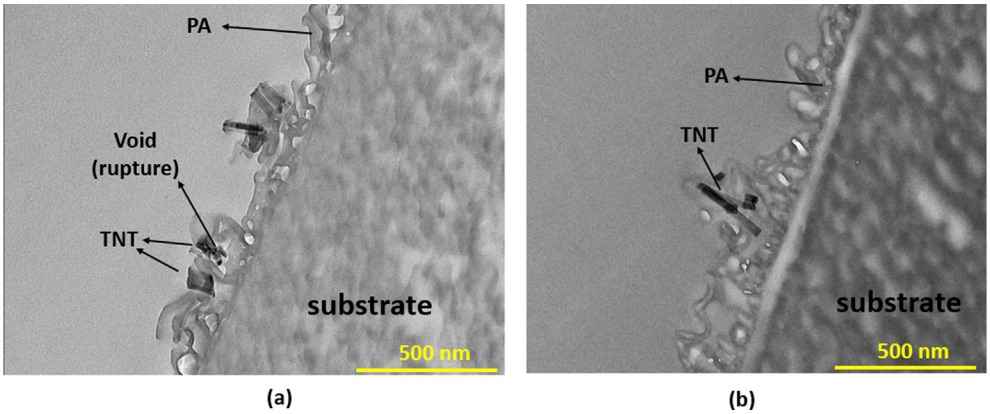


**Fig. 5.** TEM cross-sectional images of (a) TFN(5M) and (b) AA-TFN(5M) membranes.

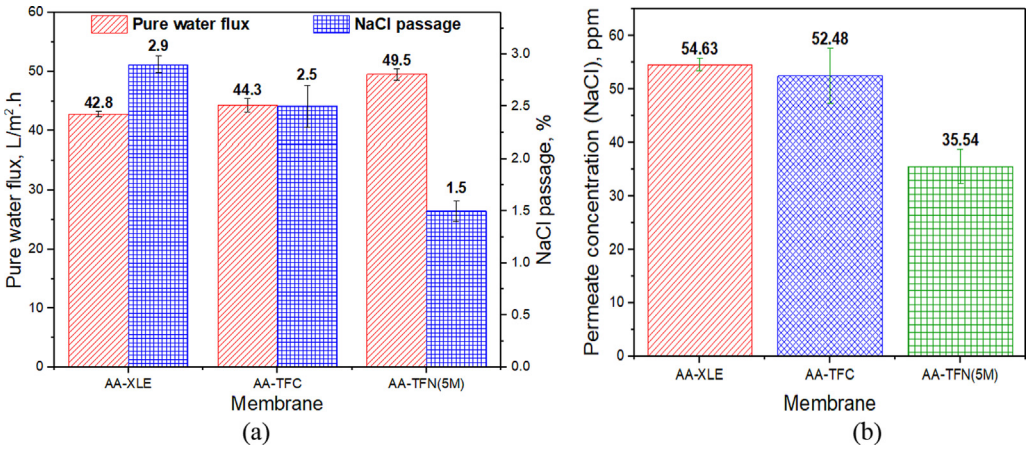


**Fig. 6.** (a) Pure water flux and NaCl passage and (b) permeate concentration (NaCl) of different AA-modified membranes tested with 2000 mg/L NaCl solution.

*Membrane antifouling properties and stability performance*

It has been generally known that improving membrane surface properties could lead to direct impact towards the membrane fouling resistance [52,53]. The membrane with higher hydrophilicity, smoother morphology and greater negative charge is more advantageous to reduce foulants deposition/adsorption [54]. As shown in Fig. 7(a), the AA-TFN(5M) membrane exhibits the smallest normalized flux decline after being used for filtration of 1000 ppm NaAlg feed solution for 5 h, indicating less foulants adsorption occurred on its modified surface. Most importantly, the presence of AA on the membrane surface also significantly improves the FRR of AA-TFN(5M) membrane (see inset in Fig. 7 (a)). Its FRR of 96.45% is much higher than the value achieved by the TFC (57.94%) and TFN(5M) membrane (85.77%). The improved surface hydrophilicity (corresponded to reduced WCA presented in

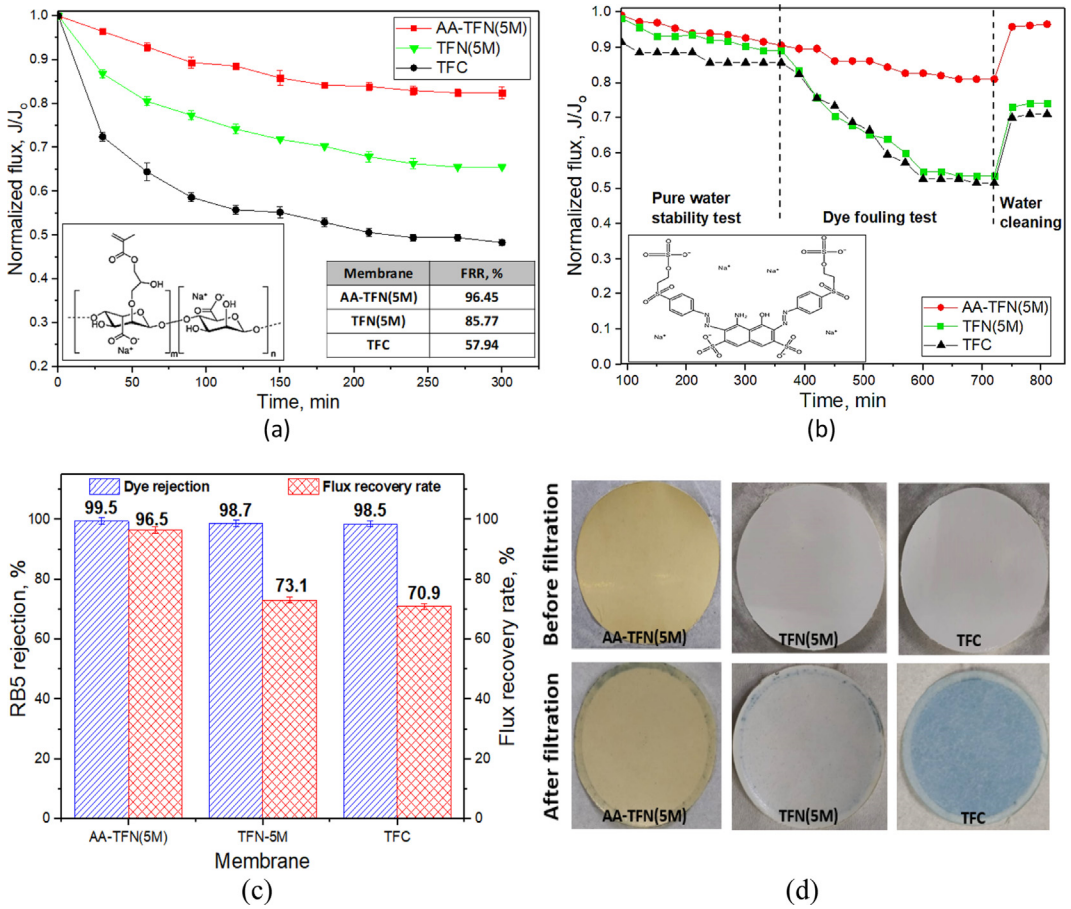


**Fig. 7.** (a) Normalized flux of membrane versus filtration time when subjected to 1000 ppm NaAlg feed solution (Inset: flux recovery rate of membranes after being cleaned by RO water and organic structure of NaAlg), (b) normalized flux of membranes as a function of time during 3-step filtration (Inset: organic structure of RB5), (i) pure water flux for 360 min, RB5 solution flux for 360 min and (iii) water flux for 100 min after cleaning with DI water, (c) RB5 rejection and flux recovery rate of membranes after being cleaned by RO water and (d) photographs of AA-TFN(5M), TFN(5M) and TFC membranes before and after filtration of 1000-ppm RB5 feed solution at 15 bar.

Fig. 4) after AA deposition plays an important role in enhancing membrane fouling resistance as it promotes hydrogen bonding between membrane surface and water molecules and develops protective hydrated layer that reduces the foulants deposited atop the PA layer [49].

With respect to the stability performance, the TFN(5M) and AA-TFN(5M) membranes are monitored via 3-step filtration using different types of feed solutions and the results are presented in Fig. 7 (b). For the TFN membrane performance, the abscission of inorganic nanomaterials is always the main concern to the researchers [19]. Compared to the TFC and TFN(5M) membrane, the flux change of the AA-TFN(5M) membrane is found to be quite stable during 360-min RB5 solution filtration. By taking into account that all these membranes possess very similar RB5 rejection (at least 98.5%, Fig. 7(c)), the smallest flux deterioration degree of the AA-TFN(5M) membrane coupled with its highest FRR could be mainly attributed to its improved surface chemistry that minimizes the adsorption and deposition of foulants. Such mechanism is important to delay the formation of irreversible foulants on the membrane surface and prolong its lifespan. Fig. 7(d) clearly shows that the dye stained on the AA-TFN(5M) membrane is apparently less in comparison to the TFN(5M) and TFC membranes, indicating the positive effect of AA-modified layer in overcoming the fouling issue. It is believed that the modified membrane with AA deposition could sustain prolonged operating condition due to the specific interaction of –OH groups of TNTs that strongly bounded with –COOH groups of PA and AA via hydrogen bonding, which possibly reduce the tendency of TNTs leaching [55,56]. On the other hand, the increased membrane surface negative charges upon AA deposition (Figure S5) could effectively repel the negatively charged pigment (RB5), resulting in higher dye rejection and reducing adhesion of foulants onto the membrane [57].

*Membrane leaching performance*

The nanofillers leaching test was further conducted for two selected membranes, i.e., TFN(5M) and AA-TFN(5M) membranes. As shown in Figure S6, the Ti contents detected in the feed and permeate samples of the AA-TFN(5M) membrane are lower compared to the TFN(5M) membrane. For the AA-TFN(5M) membrane, it is found that the average Ti content found in the feed and permeate samples throughout the operation period is ~0.5 ppb. As a comparison, the water samples of TFN(5M) membrane contain average of 1.48 ppb and 2.13 ppb for its feed and permeate, respectively. The leaching of nanofillers for both membranes could happen due to the weak interaction of some TNTs within the PA layer, but its leaching degree could be greatly minimized through surface deposition. The –COOH groups of AA coating layer on the AA-TFN(5M) membrane could have specific interaction with the –OH groups of TNT via hydrogen bonding. This, as a result, potentially reduces the detachment of TNT during operation.

## Conclusions

In this study, a green approach based on PECVD technique was utilized to modify not only the surface properties of TNTs but also the physicochemical properties of PA layer of TFN membrane incorporating functionalized TNTs. The research work aimed to heal the surface imperfections formed during IP process to produce a defect-free TFN membrane with better PA integrity and characteristics. The filtration performances of the AA-TFC and AA-TFN (5M) membranes were determined along with the commercial RO membrane (AA-XLE) and the changes in the membrane surface properties were instrumentally characterized. Compared to the AA-XLE and AA-TFC membrane, the AA-TFN(5M) membrane exhibited remarkable pure water flux and low NaCl passage as well as comparable anti-fouling ability, which is ascribed to the enhanced membrane surface hydrophilicity upon the embedment of TNTs. The AA-TFN(5M) membrane also outperformed the unmodified TFN(5M) membrane with respect to antifouling property and FRR owing to better surface hydrophilicity (reduced WCA) upon PAA plasma deposition. In conclusion, our proposed PECVD method provides an effective surface functionalization to alter the characteristics of TNTs before it was used for TFN membrane fabrication and further heal the surface imperfections of the TNTs-incorporated TFN membrane via hydrophilic coating to produce a defect-free PA nanocomposite layer with higher degree of hydrophilicity for improved desalination process.

## CRediT authorship contribution statement

**Ying Siew Khoo:** Investigation, Writing - original draft. **Woei Jye Lau:** Project administration, Supervision, Writing - review & editing. **Yong Yeow Liang:** Supervision, Writing - review & editing. **Mustafa Karaman:** Conceptualization, Methodology. **Mehmet Gürsoy:** Conceptualization, Methodology. **Ahmad Fauzi Ismail:** Supervision.

## Declaration of Competing Interest

The authors declare that they have no known competing financial interests or personal relationships that could have appeared to influence the work reported in this paper.

## Acknowledgement

This work is supported and financially funded by the Ministry of Science, Technology and Innovation (MOSTI) Malaysia under International Collaboration Fund (Grant number: IF1118I1041/R.J 130000.7951.4S143).

## Compliance with ethics requirements

This article does not contain any studies with human or animal subjects.

## Appendix A. Supplementary material

Supplementary data to this article can be found online at https://doi.org/10.1016/j.jare.2021.06.011.

## References

[1] Jeong B-H, Yan Y, Ghosh AK, Huang X, Subramani A, Hoek EMV, et al. Interfacial polymerization of thin film nanocomposites: A new concept for reverse osmosis membranes. J Memb Sci 2007;294:1–7. doi: https://doi.org/10.1016/j.memsci.2007.02.025.

[2] Lee TH, Roh JS, Yoo SY, Roh JM, Choi TH, Park HB. High-Performance Polyamide Thin-Film Nanocomposite Membranes Containing ZIF-8/CNT Hybrid Nanofillers for Reverse Osmosis Desalination. Ind Eng Chem Res 2019. doi: https://doi.org/10.1021/acs.iecr.9b04810.

[3] Ji Y, Qian W, Yu Y, An Q, Liu L, Zhou Y, et al. Recent developments in nanofiltration membranes based on nanomaterials. Chinese J Chem Eng 2017;25:1639–52. doi: https://doi.org/10.1016/J.CJCHE.2017.04.014.

[4] Lai GS, Lau WJ, Goh PS, Karaman M, Gürsoy M, Ismail AF. Development of thin film nanocomposite membrane incorporated with plasma enhanced chemical vapor deposition-modified hydrous manganese oxide for nanofiltration process. Compos Part B 2019;176:. doi: https://doi.org/10.1016/j.compositesb.2019.107328107328.

[5] Mayyahi AAl, Deng B. Efficient water desalination using photo-responsive ZnO polyamide thin film nanocomposite membrane. Environ Chem Lett 2018;16:1469–75. doi: https://doi.org/10.1007/s10311-018-0758-z.

[6] Zheng J, Li M, Yu K, Hu J, Zhang X, Wang L. Sulfonated multiwall carbon nanotubes assisted thin-film nanocomposite membrane with enhanced water flux and anti-fouling property. J Memb Sci 2017;524:344–53. doi: https://doi.org/10.1016/J.MEMSCI.2016.11.032.

[7] Chae HR, Lee J, Lee CH, Kim IC, Park PK. Graphene oxide-embedded thin-film composite reverse osmosis membrane with high flux, anti-biofouling, and chlorine resistance. J Memb Sci 2015;483:128–35. doi: https://doi.org/10.1016/j.memsci.2015.02.045.
[8] Ali MEA, Wang L, Wang X, Feng X. Thin film composite membranes embedded with graphene oxide for water desalination. Desalination 2016;386:67–76. doi: https://doi.org/10.1016/J.DESAL.2016.02.034.
[9] Isawi H, El-Sayed MH, Feng X, Shawky H, Abdel Mottaleb MS. Surface nanostructuring of thin film composite membranes via grafting polymerization and incorporation of ZnO nanoparticles. Appl Surf Sci 2016;385:268–81. doi: https://doi.org/10.1016/j.apsusc.2016.05.141.
[10] Shao F, Xu C, Ji W, Dong H, Sun Q, Yu L, et al. Layer-by-layer self-assembly TiO2 and graphene oxide on polyamide reverse osmosis membranes with improved membrane durability. Desalination 2017;423:21–9. doi: https://doi.org/10.1016/J.DESAL.2017.09.007.
[11] Kim HJ, Baek Y, Choi K, Kim DG, Kang H, Choi YS, et al. The improvement of antibiofouling properties of a reverse osmosis membrane by oxidized CNTs. RSC Adv 2014;4:32802–10. doi: https://doi.org/10.1039/c4ra06489e.
[12] Ng ZC, Lau WJ, Matsuura T, Ismail AF. Thin film nanocomposite RO membranes: Review on fabrication techniques and impacts of nanofiller characteristics on membrane properties. Chem Eng Res Des 2021;165:81–105. doi: https://doi.org/10.1016/j.cherd.2020.10.003.
[13] Liu Q, Xu GR. Graphene oxide (GO) as functional material in tailoring polyamide thin film composite (PA-TFC) reverse osmosis (RO) membranes. Desalination 2016;394:162–75. doi: https://doi.org/10.1016/j.desal.2016.05.017.
[14] Park SH, Kim SH, Park SJ, Ryoo S, Woo K, Lee JS, et al. Direct incorporation of silver nanoparticles onto thin-film composite membranes via arc plasma deposition for enhanced antibacterial and permeation performance. J Memb Sci 2016;513:226–35. doi: https://doi.org/10.1016/j.memsci.2016.04.013.
[15] Yin J, Deng B. Polymer-matrix nanocomposite membranes for water treatment. J Memb Sci 2015;479:256–75. doi: https://doi.org/10.1016/j.memsci.2014.11.019.
[16] Yang Z, Sun P-F, Li X, Gan B, Wang L, Song X, et al. A Critical Review on Thin-Film Nanocomposite Membranes with Interlayered Structure: Mechanisms, Recent Developments, and Environmental Applications. Environ Sci Technol 2020. doi: https://doi.org/10.1021/acs.est.0c05377.
[17] Lai GS, Lau WJ, Gray SR, Matsuura T, Jamshidi Gohari R, Subramanian MN, et al. A practical approach to synthesize polyamide thin film nanocomposite (TFN) membranes with improved separation properties for water/wastewater treatment. J Mater Chem A 2016;4:4134–44. doi: https://doi.org/10.1039/c5ta09252c.
[18] Al Aani S, Haroutounian A, Wright CJ, Hilal N. Thin Film Nanocomposite (TFN) membranes modified with polydopamine coated metals/carbon-nanostructures for desalination applications. Desalination 2018;427:60–74. doi: https://doi.org/10.1016/j.desal.2017.10.011.
[19] Lau WJ, Gray S, Paul Chen J, Emadzadeh D, Matsuura T, Ismail AF. A review on polyamide thin film nanocomposite (TFN) membranes: History, applications, challenges and approaches. Water Res 2015;80:306–24. doi: https://doi.org/10.1016/j.watres.2015.04.037.
[20] Liu H, Zhang M, Zhao H, Jiang Y, Liu G, Gao J. Enhanced dispersibility of metal-organic frameworks (mofs) in the organic phase: Via surface modification for tfn nanofiltration membrane preparation. RSC Adv 2020;10:4045–57. doi: https://doi.org/10.1039/c9ra09672h.
[21] Emadzadeh D, Lau WJ, Rahbari-Sisakht M, Daneshfar A, Ghanbari M, Mayahi A, et al. A novel thin film nanocomposite reverse osmosis membrane with superior anti-organic fouling affinity for water desalination. Desalination 2015;368:106–13. doi: https://doi.org/10.1016/J.DESAL.2014.11.019.
[22] Dong H, Zhao L, Zhang L, Chen H, Gao C, Winston Ho WS. High-flux reverse osmosis membranes incorporated with NaY zeolite nanoparticles for brackish water desalination. J Memb Sci 2015;476:373–83. doi: https://doi.org/10.1016/J.MEMSCI.2014.11.054.
[23] Ghanbari M, Emadzadeh D, Lau WJ, Matsuura T, Ismail AF. Synthesis and characterization of novel thin film nanocomposite reverse osmosis membranes with improved organic fouling properties for water desalination. RSC Adv 2015;5:21268–76. doi: https://doi.org/10.1039/c4ra16177g.
[24] Chong CY, Lau WJ, Yusof N, Lai GS, Ismail AF. Roles of nanomaterial structure and surface coating on thin film nanocomposite membranes for enhanced desalination. Compos Part B Eng 2019;160:471–9. doi: https://doi.org/10.1016/J.COMPOSITESB.2018.12.034.
[25] Wang S, Wen S, Shen M, Guo R, Cao X, Wang J, et al. Aminopropyltriethoxysilane-mediated surface functionalization of hydroxyapatite nanoparticles: synthesis, characterization, and in vitro toxicity assay. Int J Nanomedicine 2011;6:3449–59.
[26] Louie JS, Pinnau I, Ciobanu I, Ishida KP, Ng A, Reinhard M. Effects of polyether–polyamide block copolymer coating on performance and fouling of reverse osmosis membranes. J Memb Sci 2006;280:762–70. doi: https://doi.org/10.1016/J.MEMSCI.2006.02.041.
[27] Khoo YS, Lau WJ, Liang YY, Karaman M, Gürsoy M, Lai GS, et al. Rapid and Eco-Friendly Technique for Surface Modification of TFC RO Membrane for Improved Filtration Performance. J Environ Chem Eng 2021;9:. doi: https://doi.org/10.1016/j.jece.2021.105227105227.
[28] Shan X, Li SL, Fu W, Hu Y, Gong G, Hu Y. Preparation of high performance TFC RO membranes by surface grafting of small-molecule zwitterions. J Memb Sci 2020;608:. doi: https://doi.org/10.1016/j.memsci.2020.118209118209.
[29] Shen J nan, Yu C chao, Ruan H min, Gao C jie, Van der Bruggen B. Preparation and characterization of thin-film nanocomposite membranes embedded with poly(methyl methacrylate) hydrophobic modified multiwalled carbon nanotubes by interfacial polymerization. J Memb Sci 2013;442:18–26. https://doi.org/10.1016/J.MEMSCI.2013.04.018.
[30] Hassan MM, Carr CM. A review of the sustainable methods in imparting shrink resistance to wool fabrics. J Adv Res 2019;18:39–60. doi: https://doi.org/10.1016/j.jare.2019.01.014.
[31] Wang J, Chen X, Reis R, Chen Z, Milne N, Winther-Jensen B, et al. Plasma modification and synthesis of membrane materials—a mechanistic review. Membranes (Basel) 2018. doi: https://doi.org/10.3390/membranes8030056.
[32] Khoo YS, Lau WJ, Liang YY, Karaman M, Gürsoy M, Ismail AF. A Green Approach to Modify Surface Properties of Polyamide Thin Film Composite Membrane for Improved Antifouling Resistance. Sep Purif Technol 2020:116976. https://doi.org/10.1016/j.seppur.2020.116976.
[33] Subramaniam MN, Goh PS, Lau WJ, Ismail AF, Gürsoy M, Karaman M. Synthesis of Titania nanotubes/polyaniline via rotating bed-plasma enhanced chemical vapor deposition for enhanced visible light photodegradation. Appl Surf Sci 2019;484:740–50. doi: https://doi.org/10.1016/J.APSUSC.2019.04.118.
[34] Gürsoy M, Karaman M. Hydrophobic coating of expanded perlite particles by plasma polymerization. Chem Eng J 2016;284:343–50. doi: https://doi.org/10.1016/J.CEJ.2015.09.007.
[35] Khoo YS, Seah MQ, Lau WJ, Liang YY, Karaman M, Gürsoy M, et al. Environmentally Friendly Approach for the Fabrication of Polyamide Thin Film Nanocomposite Membrane with Enhanced Antifouling and Antibacterial Properties. Sep Purif Technol 2020;260:. doi: https://doi.org/10.1016/j.seppur.2020.118249118249.
[36] Khoo YS, Lau WJ, Chamani H, Matsuura T, Ismail AF. Water flux increase by inverting the membrane from its normal position – Is it occurring in FO and PRO?. J Water Process Eng 2020;37:. doi: https://doi.org/10.1016/j.jwpe.2020.101366101366.
[37] Ang MBMY, Huang S-H, Chang M-W, Lai C-L, Tsai H-A, Hung W-S, et al. Ultraviolet-initiated graft polymerization of acrylic acid onto thin-film polyamide surface for improved ethanol dehydration performance of pervaporation membranes. Sep Purif Technol 2020;235:. doi: https://doi.org/10.1016/J.SEPPUR.2019.116155116155.
[38] Xie W, Geise GM, Freeman BD, Lee HS, Byun G, McGrath JE. Polyamide interfacial composite membranes prepared from m-phenylene diamine, trimesoyl chloride and a new disulfonated diamine. J Memb Sci 2012;403–404:152–61. doi: https://doi.org/10.1016/j.memsci.2012.02.038.
[39] Ma R, Ji YL, Weng XD, An QF, Gao CJ. High-flux and fouling-resistant reverse osmosis membrane prepared with incorporating zwitterionic amine monomers via interfacial polymerization. Desalination 2016;381:100–10. doi: https://doi.org/10.1016/j.desal.2015.11.023.
[40] Liu Q, Xie L, Du H, Xu S, Du Y. Study on the concentration of acrylic acid and acetic acid by reverse osmosis. Membranes (Basel) 2020;10:1–13. doi: https://doi.org/10.3390/membranes10070142.
[41] Abbas MA, Mushtaq S, Cheema WA, Qiblawey H, Zhu S, Li Y, et al. Surface Modification of TFC-PA RO Membrane by Grafting Hydrophilic pH Switchable Poly(Acrylic Acid) Brushes. Adv Polym Technol 2020;2020:1–12. doi: https://doi.org/10.1155/2020/8281058.
[42] Lai GS, Lau WJ, Goh PS, Tan YH, Ng BC, Ismail AF. A novel interfacial polymerization approach towards synthesis of graphene oxide-incorporated thin film nanocomposite membrane with improved surface properties. Arab J Chem 2019;12:75–87. doi: https://doi.org/10.1016/J.ARABJC.2017.12.009.
[43] Shen H, Wang S, Xu H, Zhou Y, Gao C. Preparation of polyamide thin film nanocomposite membranes containing silica nanoparticles via an in-situ polymerization of SiCl4 in organic solution. J Memb Sci 2018;565:145–56. doi: https://doi.org/10.1016/j.memsci.2018.08.016.
[44] Yin J, Zhu G, Deng B. Graphene oxide (GO) enhanced polyamide (PA) thin-film nanocomposite (TFN) membrane for water purification. Desalination 2016;379:93–101. doi: https://doi.org/10.1016/J.DESAL.2015.11.001.
[45] Emadzadeh D, Lau WJ, Rahbari-Sisakht M, Ilbeygi H, Rana D, Matsuura T, et al. Synthesis, modification and optimization of titanate nanotubes-polyamide thin film nanocomposite (TFN) membrane for forward osmosis (FO) application. Chem Eng J 2015;281:243–51. doi: https://doi.org/10.1016/J.CEJ.2015.06.035.
[46] Ahmad NA, Goh PS, Wong KC, Zulhairun AK, Ismail AF. Enhancing desalination performance of thin film composite membrane through layer by layer assembly of oppositely charged titania nanosheet. Desalination 2020;476:. doi: https://doi.org/10.1016/J.DESAL.2019.114167114167.
[47] Yu S, Yao G, Dong B, Zhu H, Peng X, Liu J, et al. Improving fouling resistance of thin-film composite polyamide reverse osmosis membrane by coating natural hydrophilic polymer sericin. Sep Purif Technol 2013;118:285–93. doi: https://doi.org/10.1016/j.seppur.2013.07.018.
[48] Vatanpour V, Zoqi N. Surface modification of commercial seawater reverse osmosis membranes by grafting of hydrophilic monomer blended with carboxylated multiwalled carbon nanotubes. Appl Surf Sci 2017;396:1478–89. doi: https://doi.org/10.1016/J.APSUSC.2016.11.195.
[49] Zou L, Vidalis I, Steele D, Michelmore A, Low SP, Verberk JQJC. Surface hydrophilic modification of RO membranes by plasma polymerization for low organic fouling. J Memb Sci 2011;369:420–8. doi: https://doi.org/10.1016/j.memsci.2010.12.023.
[50] Ni L, Meng J, Li X, Zhang Y. Surface coating on the polyamide TFC RO membrane for chlorine resistance and antifouling performance improvement.

J Memb Sci 2014;451:205–15. doi: https://doi.org/10.1016/J.MEMSCI.2013.09.040.
[51] Sun J, Zhu LP, Wang ZH, Hu F, Bin Zhang P, Zhu BK. Improved chlorine resistance of polyamide thin-film composite membranes with a terpolymer coating. Sep Purif Technol 2016;157:112–9. doi: https://doi.org/10.1016/j.seppur.2015.11.034.
[52] Kang G dong, Cao Y ming. Development of antifouling reverse osmosis membranes for water treatment: A review. Water Res 2012;46:584–600. https://doi.org/10.1016/j.watres.2011.11.041.
[53] Ishigami T, Amano K, Fujii A, Ohmukai Y, Kamio E, Maruyama T, et al. Fouling reduction of reverse osmosis membrane by surface modification via layer-by-layer assembly. Sep Purif Technol 2012;99:1–7. doi: https://doi.org/10.1016/j.seppur.2012.08.002.
[54] Kochkodan VM, Sharma VK. Graft polymerization and plasma treatment of polymer membranes for fouling reduction: A review. J Environ Sci Heal - Part A Toxic/Hazardous Subst Environ Eng 2012;47:1713–27. doi: https://doi.org/10.1080/10934529.2012.689183.
[55] Lee HS, Kim JH, Min BR, Lee HS, Kim JP, Im SJ, et al. Polyamide thin-film nanofiltration membranes containing TiO2 nanoparticles. Desalination 2007;219:48–56. doi: https://doi.org/10.1016/j.desal.2007.06.003.
[56] Kim SH, Kwak S-Y, Sohn B-H, Park TH. Design of TiO2 nanoparticle self-assembled aromatic polyamide thin-film-composite (TFC) membrane as an approach to solve biofouling problem. J Memb Sci 2003;211:157–65. doi: https://doi.org/10.1016/S0376-7388(02)00418-0.
[57] Alventosa-Delara E, Barredo-Damas S, Zuriaga-Agustí E, Alcaina-Miranda MI, Iborra-Clar MI. Ultrafiltration ceramic membrane performance during the treatment of model solutions containing dye and salt. Sep Purif Technol 2014;129:96–105. doi: https://doi.org/10.1016/j.seppur.2014.04.001.